

Jahn-Teller polarons and their superconductivity in a molecular conductor

R. Ramakumar and Sudhakar Yarlagadda

Condensed Matter Physics Group, Saha Institute of Nuclear Physics, 1/AF Bidhannagar, Calcutta-700064, INDIA
(29 July 2003)

We present a theoretical study of a possibility of superconductivity in a three dimensional molecular conductor in which the interaction between electrons in doubly degenerate molecular orbitals and an *intramolecular* vibration mode is large enough to lead to the formation of $E \otimes \beta$ Jahn-Teller small polarons. We argue that the effective polaron-polaron interaction can be attractive for material parameters realizable in molecular conductors. This interaction is the source of superconductivity in our model. On analyzing superconducting instability in the weak and strong coupling regimes of this attractive interaction, we find that superconducting transition temperatures up to 100 K are achievable in molecular conductors within this mechanism. We also find, for two particles per molecular site, a novel Mott insulating state in which a polaron singlet occupies one of the doubly degenerate orbitals on each site. Relevance of this study in the search for new molecular superconductors is pointed out.

PACS numbers: 74.70Kn, 74.20.Fg, 63.20.Kr, 74.20Mn

I. INTRODUCTION

Ever since the experimental discovery¹ of superconductivity by Jerome *et al.*, in 1980 in a Bechgaard² salt (TMTTF)₂PF₆ (with a T_c of 1.2 K under a pressure of 6.5 Kbar), search for new higher T_c molecular superconductors has been a vigorous field of research³. A large number of molecular superconductors³ with varying degrees of dimensionality have been discovered since 1980, and a continuing multidisciplinary search for new higher T_c molecular superconductors is currently underway. Theoretical studies of a possibility of superconductivity in molecular conductors and conducting polymers have had a positive influence in the development of this field. Indeed, Little's⁴ prediction of high superconducting transition temperatures within an exciton mediated mechanism of superconductivity in a hypothetical conducting polymer chain (with polarizable molecules periodically attached to the spine) played a boosting role for this field⁵. For a discussion on the future prospects for superconductivity in conducting polymers see Heeger⁶.

One of the strategies in the search for higher T_c molecular superconductors continues to be to search for molecules with large electron-*intramolecular* vibration coupling (EMVC) and to crystallize them with the hope that the solid will be metallic or can be made metallic by charge transfer from another molecule (in charge-transfer salts) and/or by application of pressure. If the material is metallic and if EMVC is the pairing glue, large EMVC implies a large T_c within the framework of BCS theory⁷. In a molecular conductor, the phonon spectrum forms two distinct groups: high-frequency *intramolecular* phonons and *intermolecular* phonons which have relatively low frequencies ($< 300 \text{ cm}^{-1}$ in the currently known organic superconductors). Where calculations are available⁸, the EMVC's are larger than the electron-*intermolecular* vibration coupling, though there are exceptions to this trend⁹. But, when EMVC's be-

come large, there is a possibility of polaron formation¹⁰, a possibility not included in the Migdal-Eliashberg^{11,12} extension of the BCS theory. If EMVC is large enough to lead to small polaron formation, a possibility for superconductivity to arise is by the polaron pairing through the exchange of low frequency *intermolecular* phonons. Recently we investigated¹⁴ this possibility in a simple model molecular conductor. In that work we considered molecular orbitals, overlaps of which on nearest neighbor (NN) molecules produces the conduction band, to have *no orbital degeneracy*.

Now, depending on the symmetry of the molecule, the molecular orbitals which participate in the band formation can be degenerate or non-degenerate. The purpose of the present paper is to investigate the possibility of superconductivity in a three dimensional molecular conductor in which the molecular orbitals participating in the conduction band formation are doubly degenerate and EMVC between electrons and a single *intramolecular* vibration mode is large enough to lead to the formation of Jahn-Teller (JT) small polarons. This is the $E \otimes \beta$ JT model and is the simplest JT system. Molecules with tetragonal symmetry are examples of such a system.

The rest of the paper is organized as follows. In Sec. II, we introduce our model for the molecular conductor, perform a Lang-Firsov transformation on it to obtain the JT polaron Hamiltonian. In Sec. III, a BCS-mean-field (BCS-MF) theory is presented which is applicable in the weak coupling regime of the effective attractive interaction between the JT small polarons. In Sec. IV, we analyze the strong coupling Bose regime. An insulating state obtained for the case of two electrons per site is discussed in Sec. V. The conclusions are given in Sec. VI.

II. JAHN-TELLER SMALL POLARONS AND THEIR EFFECTIVE INTERACTIONS

We employ the following model to study the $E \otimes \beta$ JT polaron formation and their effective interactions:

$$\begin{aligned}
H = & t \sum_{ij} \sum_{\alpha\sigma} c_{i\alpha\sigma}^\dagger c_{j\alpha\sigma} + \omega \sum_{\mathbf{q}} b_{\mathbf{q}}^\dagger b_{\mathbf{q}} \\
& + \frac{G}{\sqrt{N}} \sum_{j\mathbf{q}\sigma} (n_{j1\sigma} - n_{j2\sigma}) e^{i\mathbf{q} \cdot \mathbf{R}_j} (b_{-\mathbf{q}}^\dagger + b_{\mathbf{q}}) \\
& + U \sum_{j\alpha} n_{j\alpha\uparrow} n_{j\alpha\downarrow} + U \sum_{j\sigma\sigma'} n_{j1\sigma} n_{j2\sigma'}. \quad (1)
\end{aligned}$$

In the above H , i and j are the molecular site indices, α ($=1, 2$) is the orbital index of the two degenerate molecular orbitals, t (< 0) the hopping energy between similar orbitals on NN molecules, ω the molecular vibration frequency, G the electron-phonon (*el-ph*) interaction energy, M the mass, U the Coulomb interaction strength, and N the number of sites. Furthermore, $c_{j\alpha\sigma}$ and $b_{\mathbf{q}}$ are the destruction operators of electrons and phonons respectively, and $n_{j\alpha\sigma} = c_{j\alpha\sigma}^\dagger c_{j\alpha\sigma}$. A chemical potential will be introduced later when we have to fix the electron density. In the Appendix, using an argument given in Ref.¹⁵ we show that, for $2G/\omega \gg 1$, the $E \otimes e$ JT model reduces to $E \otimes \beta$ JT model. A detailed numerical study of polaron and bipolaron formation in $E \otimes e$ JT model in one dimension and for the case of one and two electrons was recently published by Shawish *et.al.*¹⁶.

Our calculation proceeds along the following lines. First we apply a multi-band Lang-Firsov (LF) transformation¹⁷ which produces the JT small polarons, reduces the *intraorbital* Coulomb repulsion, and increases the *interorbital* Coulomb repulsion. We will argue that the *intraorbital* polaron-polaron interaction can be attractive for realistic range of frequencies and *el-ph* coupling realizable in molecular conductors. This interaction then is the source of superconductivity in our model. In the next step, we project out *interorbital* double occupancies employing a Gutzwiller approximation¹⁸ method in the weak and strong coupling regimes of the attractive interaction to obtain effective Hamiltonians in these regimes. These effective JT Hamiltonians are used to study superconductivity in the weak-coupling BCS-MF and strong-coupling (Bose) regimes. The superconducting transition temperatures obtained are then analyzed as a function of phonon frequency, *el-ph* interaction strength, Coulomb repulsion strength, original band-width, and doping. We will also see that, for the case of two polarons per site, we obtain a novel insulating state with a polaron singlet occupying the lattice sites. For this paired polaron Mott insulator, we show that one obtains a novel Orbital Density Wave State (ODW) for large and finite *interorbital* repulsion. We also point out a mapping of this ODW state to the Ising model. From our analysis of the superconducting transition temperature in the BCS-MF regime and the Bose regime, it

will be shown that superconducting T_c up to 100 K is achievable for this mechanism. Now we go to the details of the calculations.

As stated, we apply a multi-band LF transformation to the H . The transformation $e^S H e^{-S} = H_T$ transforms H into the polaron representation. LF is a unitary transformation with $S = S_1 + S_2$, where S_α ($\alpha = 1, 2$) is

$$S_\alpha = (-1)^\alpha \frac{G}{\omega} \frac{1}{\sqrt{N}} \sum_{j\mathbf{q}\sigma} n_{j\alpha\sigma} e^{i\mathbf{q} \cdot \mathbf{R}_j} (b_{\mathbf{q}} - b_{-\mathbf{q}}^\dagger). \quad (2)$$

Using this S , we have

$$e^S b_{\mathbf{q}}^\dagger e^{-S} = b_{\mathbf{q}}^\dagger - \frac{G}{\omega} \frac{1}{\sqrt{N}} \sum_{j\sigma} (n_{j1\sigma} - n_{j2\sigma}) e^{i\mathbf{q} \cdot \mathbf{R}_j}, \quad (3)$$

$$e^S c_{j\alpha\sigma} e^{-S} = e^{S_\alpha} c_{j\alpha\sigma} e^{-S_\alpha} = c_{j\alpha\sigma} X_{j\alpha}, \quad (4)$$

and

$$X_{j\alpha} = \exp \left[(-1)^{\alpha-1} \frac{G}{\omega} \frac{1}{\sqrt{N}} \sum_{\mathbf{q}} e^{i\mathbf{q} \cdot \mathbf{R}_j} (b_{\mathbf{q}} - b_{-\mathbf{q}}^\dagger) \right]. \quad (5)$$

Using the above operators, the transformed Hamiltonian is

$$H_T = H_{KE} + H_R + H_A + H_I, \quad (6)$$

where

$$H_{KE} = t \sum_{ij} \sum_{\alpha\sigma} c_{i\alpha\sigma}^\dagger c_{j\alpha\sigma} X_{i\alpha}^\dagger X_{j\alpha}, \quad (7)$$

$$H_R = U_R \sum_{j\sigma\sigma'} n_{j1\sigma} n_{j2\sigma'}, \quad (8)$$

$$H_A = U_A \sum_{j\alpha} n_{j\alpha\uparrow} n_{j\alpha\downarrow}, \quad (9)$$

and

$$H_I = \omega \sum_{\mathbf{q}} b_{\mathbf{q}}^\dagger b_{\mathbf{q}} - \frac{G^2}{\omega} \sum_{j\alpha\sigma} n_{j\alpha\sigma}. \quad (10)$$

In the above equations

$$U_R = U + 2 \frac{G^2}{\omega}, \quad (11)$$

and

$$U_A = U - 2 \frac{G^2}{\omega}. \quad (12)$$

The LF transformation produces three effects. The first is the polaronic band-width reduction, of course. The

second and third effects are the enhancement of the *interorbital* Coulomb repulsion and the reduction of the *intraorbital* Coulomb repulsion, respectively. These second and third effects have different origins: while the second has its origin in the JT nature of the system, the third is a small polaron effect. On phonon averaging¹⁹ of H_T as usual, neglecting a constant coming from H_I , one obtains

$$H_P = H_{KE}^P + H_R + H_A, \quad (13)$$

where

$$H_{KE}^P = t_P \sum_{ij} \sum_{\alpha\sigma} c_{i\alpha\sigma}^\dagger c_{j\alpha\sigma}, \quad (14)$$

in which

$$t_P = t \times \exp \left[- \left(\frac{G}{\omega} \right)^2 \coth \left(\frac{\beta\omega}{2} \right) \right], \quad (15)$$

and $\beta = 1/k_B T$.

Now, H_P is the Hamiltonian for a collection of JT small polarons and these polarons interact among themselves though in the *intra* and *inter* orbital interactions U_A and U_R , respectively. At this stage, we demand that U_A be an attractive interaction. This is very much realizable for the values of U , G , and ω in a range possible in molecular conductors. Some idea about the range of U , G , and ω would be useful to get a better feel. The highest *intramolecular* vibration frequency is unlikely to exceed the frequency (4161 cm^{-1}) of the lightest molecule (H_2 , the Hydrogen molecule). Among the calculated values²⁰ of G , the highest seems to be around 200 meV (obtained for a mode of frequency 1656 cm^{-1} in Benzene). Practically all the existing molecular superconductors are built from the molecules TMTSF, BEDT-TTF, DMIT, DMET, BETS, or C_{60} . This is arguably a small subset of already synthesizable molecules. Then, it is quite possible that higher values of G are realized in many molecules. As for U , large and highly polarizable molecules can be expected to have small U 's. In the existing molecular superconductors³, U seems to be in a range around 1 eV. We note that the U is *not* for an isolated molecule, but for a molecule sitting on a lattice site in the solid so that U includes the effects of polarization of molecules surrounding a given molecule and consequently is reduced from the U value for the isolated molecule. Now, if we tentatively fix an upper limit for G around 600 meV and keep the upper limit of ω as 4161 cm^{-1} , it is not unreasonable to expect U_A to be negative in a range of U which obtains in molecular conductors. Given the estimates of *el-ph* coupling to individual modes, this situation is very unlikely to be realized in the existing organic superconductors. But, that does not preclude its realizability in another important class of materials: the molecular conductors yet to be discovered. In our study, we assume that U_A is negative. This attractive U_A is then the origin of superconductivity in our theory. In the next two sections, we study superconductivity in the weak and strong coupling regimes of U_A .

III. BCS MEAN-FIELD THEORY IN THE WEAK COUPLING REGIME OF U_A

The weak coupling regime of U_A is the range of U_A in which the superconducting T_c and the pair formation temperature are the same. In this section, we project out *interorbital* double occupancies, using the Gutzwiller approximation method, to obtain an effective Hamiltonian in the weak coupling regime of U_A and then study the superconductivity using a BCS-MF theory. The Gutzwiller projection renormalizes t_P and U_A , and decouples the orbitals. First, we recall that the bare *el-el* repulsions [in Eq. (1)] are strongly renormalized [Eqs. (11) and (12)]: while the *interorbital* repulsions have increased, the *intraorbital* repulsion is suppressed to an extent that it has become attractive (see the previous paragraph). The effect of U_R is to strongly reduce the probability of polarons occupying different orbitals on a given site. On the other hand, U_A (now attractive) increases the probability of two polarons (with opposite spins) occupying the same orbital on a given site. Both these aspects have to be considered while doing the Gutzwiller projection. We take, for simplicity, the U_R to be infinity and completely project out the *interorbital* double occupancies. Qualitatively one can see that projecting the *interorbital* double occupancies reduces the polaron band-width (through a density dependent function) since it is energetically unfavorable for a polaron to hop from an orbital (say 1) on a site to a target site where the orbital 2 is occupied. Also, strong reduction of *interorbital* double occupancies increases the *intraorbital* double occupancies and consequently modifies the *intraorbital* attraction. We do the *interorbital* double occupancy projection in an approximate way. First consider the part $H_{KE}^P + H_R$ of H_P [Eq. (13)]. We write the Gutzwiller wave function $|\psi_{GW}\rangle$ as:

$$|\psi_{GW}\rangle = \prod_{i\sigma\sigma'} [1 - (1 - \eta)n_{i1\sigma}n_{i2\sigma'}] |\psi_\circ\rangle, \quad (16)$$

where

$$|\psi_\circ\rangle = \prod_{k_1 < k_F} c_{k_1}^\dagger |0\rangle \otimes \prod_{k_2 < k_F} c_{k_2}^\dagger |0\rangle. \quad (17)$$

For calculating the expectation value of H_{KE}^P and H_R in $|\psi_{GW}\rangle$, we use a simple intuitive method proposed by Okabe²¹. Since the maximum number of polarons ($\sum_{\alpha\sigma} n_{\alpha\sigma}$) a site can accommodate is four, there are sixteen possibilities for occupancy for finite U_R . As mentioned earlier, we take U_R infinity limit for simplicity [$\eta = 0$ in Eq. (16)], and consequently the sixteen possibilities reduces to seven. In the paramagnetic case (*i.e.*, $n_{1\uparrow} = n_{1\downarrow} = n_{2\uparrow} = n_{2\downarrow} = n/4$), the probability

for a site to be vacant is $[1 - (n - 2d)]$ and the probability for a site to be singly occupied is $(n/4 - d)$. Here d is the *intraorbital* double occupancy. Then, considering the hopping process given in Fig. 1, the Gutzwiller band narrowing factor is

$$q(n, d) = \frac{[\sqrt{(\frac{n}{4} - d)(1 - n + 2d)} + \sqrt{d(\frac{n}{4} - d)}]^2}{\frac{n}{4}(1 - \frac{n}{4})}, \quad (18)$$

where the numerator and the denominator corresponds to hopping in the presence and absence of *interorbital* repulsion, respectively. The ground state energy for $H_{KE}^P + H_R$ is

$$E_c(n, d) = q(n, d) \sum_{\alpha\sigma} \epsilon_{\alpha\sigma}, \quad (19)$$

where $\epsilon_{\alpha\sigma} [= \epsilon]$ is the average kinetic energy per polaron, and is independent of the indices α and σ . Minimization of $E_c(n, d)$ with respect to d leads to the equation to determine d for a given n :

$$8d^3 + (4 - 6n)d^2 + (1 - 2n + \frac{9}{8}n^2)d + \frac{n^3 - n^2}{16} = 0. \quad (20)$$

For $n = 2$, the above equation implies that $d = 0.5$, which means that one of the orbitals on all the sites are occupied by a singlet. For a general value of n , one has to solve Eq. (20) to obtain the variation of d as a function of n . The optimized values of the band narrowing factor $q(n, d_{opt})$ and the *intraorbital* double occupancy (d_{opt}) as a function of n are shown in Fig. 2 and Fig. 3, respectively. From the numerical results shown in the figures, we have

$$q(n) = q(n, d_{opt}) \approx \frac{2 - n}{2}, \quad (21)$$

and

$$d_{opt} \approx \frac{n^2}{8}. \quad (22)$$

Furthermore, it is clear that as $n \rightarrow 2$, the polaron bandwidths are narrowed and a Mott insulator is obtained for $n = 2$. This Mott insulator has a singlet in one of the orbitals on each lattice site. The properties and excitations of this insulator will be discussed separately in Sect. V. Next consider the term H_A in Eq. (13). To get the total ground state energy, we add to $E_c(n, d)$ the contribution from H_A obtained using $|\psi_{GW}\rangle$ calculated for optimized d (d_{opt}). This contribution per site is

$$-|U_A| \frac{\langle \psi_{GW} | \sum_{\alpha} n_{i\uparrow\alpha} n_{i\downarrow\alpha} | \psi_{GW} \rangle}{\langle \psi_{GW} | \psi_{GW} \rangle} = -2|U_A|d_{opt}. \quad (23)$$

So, the total minimized energy per site is

$$E(n) = \sum_{\alpha\sigma} q(n, d_{opt}) \epsilon_{\alpha\sigma} - 2|U_A|d_{opt}. \quad (24)$$

Using Eqs. (21) and (22), the minimized energy per site is

$$E(n) \approx 2(2 - n)\epsilon - \frac{|U_A|n^2}{4}. \quad (25)$$

Using the results of the Gutzwiller projection of interorbital double occupancies, we write an effective Hamiltonian for the JT polarons as:

$$\tilde{H}_P = q(n)t_P \sum_{ij} \sum_{\alpha\sigma} c_{i\alpha\sigma}^\dagger c_{j\alpha\sigma} + \tilde{U}_A \sum_{j\alpha} n_{j\alpha\uparrow} n_{j\alpha\downarrow}. \quad (26)$$

The effects of Gutzwiller projection are the density dependent band-width renormalization and a renormalization of the on-site *intraorbital* attractive interaction from U_A to \tilde{U}_A . From Eq. (25), it follows that $\tilde{U}_A = 2U_A$. We notice that this enhancement is similar to the enhancement of antiferromagnetic exchange interaction (J) obtained on Gutzwiller projection in a $t-U-J$ model studied in Ref²². For the $t-U-J$ model, they found that the bare J steadily increases with increasing electron density to reach $4J$ in the Mott insulator at the half-filling of their non-degenerate band. Notice also, for our model, that orbitals are decoupled on Gutzwiller projection.

Now, \tilde{H} is clearly an effective attractive Hubbard model. We note that, unlike the usual phonon mediated attractive interaction which is attractive only in the Debye shell around the Fermi surface, all the polarons experience the attraction \tilde{U}_A or U_A . In the next section, we study superconductivity in the weak coupling regime of \tilde{U}_A using a BCS type mean-field (BCS-MF) analysis to obtain superconducting energy gap and T_c .

To move forward, we have to fix the weak and strong coupling regimes of the single band attractive Hubbard model ($H_{AHM} = t \sum_{ij\sigma} c_{i\sigma}^\dagger c_{j\sigma} - |U| \sum_j n_{j\uparrow} n_{j\downarrow}$) in terms of $|U|/t$. We can approximately fix these ranges using the existing studies²³⁻²⁵ on three dimensional non-degenerate attractive Hubbard model. A comparison of results for superconducting T_c obtained using three methods (T-Matrix Approximation, Determinant Quantum Monte Carlo, and Dynamical Mean Field Theory) and the BCS-MF is given in Fig. 2 of Ref.²⁵ Notice that these results are for quarter filling of the band. The regime of weak coupling, for a given n , is the range of $|U|/t$ within which the pair formation temperature and the superconducting transition temperature are the same. Using the calculation of Pauli susceptibility (which would be suppressed above the superconducting T_c in the case pairs form above T_c), the authors of²⁵ argued that $0 < |U|/t < 4$ is the BCS-MF regime for $n = 0.5$. Considering together all these results, we tentatively fixed the BCS-MF regime of the 3D attractive Hubbard model to be $0 < |U|/t < 3$. As for the strong coupling regime, all the electrons are in paired states below a pair formation temperature of $O(|U|)$. We fixed the Bose regime to be for $|U|/t > 12$. The intermediate coupling regime

then is obviously $3 < |U|/t < 12$. In the weak coupling regime of U_A , the ratio equivalent to $|U|/t$ in our case is, from Eq. (26), $|\tilde{U}_A|/q(n)t_P$. In the strong coupling regime of U_A studied in the next section, the Gutwiller projection has to be done in a different way than that given in this section, and that gives $|U_A|/\sqrt{q(n)}t_P$ [where $\tilde{q}(n) = (1 - n/2)/(1 - n/4)$] as the ratio equivalent to $|U|/t$. We can now proceed to the analysis of superconductivity in the BCS-MF regime of the effective attractive interaction \tilde{U}_A .

We have from Eq. (26),

$$\tilde{H}_P^\alpha = \sum_{\mathbf{k}\sigma} \xi_P^\alpha(\mathbf{k}) n_{\mathbf{k}\alpha\sigma} + \tilde{U}_A \sum_j n_{j\alpha\uparrow} n_{j\alpha\downarrow}, \quad (27)$$

where

$$\xi_P^\alpha(k) = q(n)\epsilon_P^\alpha(k) - \mu, \quad (28)$$

and

$$\epsilon_P^\alpha(k) = 2t_P[\cos(k_x a) + \cos(k_y a) + \cos(k_z a)], \quad (29)$$

for a simple cubic lattice. We have introduced a chemical potential (μ) to fix the number density. Given the form of \tilde{U}_A , only isotropic s-wave pairing is possible. A BCS-MF theory of \tilde{H}_P^α gives:

$$\tilde{H}_P^\alpha = \sum_{\mathbf{k}\sigma} \xi_P^\alpha(\mathbf{k}) n_{\mathbf{k}\alpha\sigma} + \sum_{\mathbf{k}} (\Delta_\alpha^* c_{-\mathbf{k}\alpha\downarrow} c_{\mathbf{k}\alpha\uparrow} + h.c.), \quad (30)$$

where the superconducting gap parameter is

$$\Delta_\alpha^* = \tilde{U}_A \sum_{\mathbf{k}} \langle c_{\mathbf{k}\alpha\uparrow}^\dagger c_{-\mathbf{k}\alpha\downarrow}^\dagger \rangle. \quad (31)$$

The superconducting gap and the particle density is determined from

$$\frac{2}{|\tilde{U}_A|} = \int_{-q(n)D_P}^{+q(n)D_P} \frac{N_P(\epsilon^\alpha)}{q(n)} F(\epsilon^\alpha, \Delta_\alpha, \mu, \beta) d\epsilon^\alpha, \quad (32)$$

and

$$1 - n_\alpha = \int_{-q(n)D_P}^{+q(n)D_P} \frac{N_P(\epsilon^\alpha)}{q(n)} (\epsilon^\alpha - \mu) F(\epsilon^\alpha, \Delta_\alpha, \mu, \beta) d\epsilon^\alpha, \quad (33)$$

where

$$F(\epsilon^\alpha, \Delta_\alpha, \mu, \beta) = \frac{\tanh\left(0.5\beta\sqrt{(\epsilon_\alpha - \mu)^2 + |\Delta_\alpha|^2}\right)}{\sqrt{(\epsilon_\alpha - \mu)^2 + |\Delta_\alpha|^2}}. \quad (34)$$

Here $N_P(\epsilon^\alpha)$ is the polaron Density Of States (DOS) corresponding to the polaron band $\epsilon_P^\alpha(k)$. Assuming a square one-polaron single-spin DOS (*i.e.*, $N_P(\epsilon^\alpha) = 1/2D_P = 1/12t_P$), the solutions of the gap and chemical potential equations give:

$$\Delta_\alpha(T=0) = \frac{\sqrt{\frac{\delta^2}{4} - \frac{\delta^4}{16}} D_P}{\sinh\left(\frac{1}{\lambda}\right)}, \quad (35)$$

and

$$k_B T_c = \sqrt{\frac{\delta^2}{4} - \frac{\delta^4}{16}} 1.13 D_P e^{-\frac{1}{\lambda}}. \quad (36)$$

In the above equations, $\lambda = 2|U - 2g^2\omega|/(2q(n)D_P)$, $D_P = D_o e^{-g^2}$, $\delta = 2 - n$, $g = G/\omega$, and n is the number of polarons per site. For the values of g and ω we use in numerical calculations, the temperature dependence of the polaron band-width is practically nil for the temperature range (< 300 K) of interest to us. The equation for T_c is valid for $[(q(n)D_P \pm \mu)/k_B T_c] \gg 1$. See also the note in Ref²⁶.

Now we go to the estimates of $\Delta_\alpha(0)$ and T_C considering realistic values of g , ω , D_o , and U applicable to molecular conductors. While making the estimates, one has to satisfy several constraints. These are: (i) JT small polaron formation condition ($g^2\omega > q(n)D_o$); (ii) Phonon frequency should be below the frequency (4161 cm^{-1}) of the lightest molecule (H_2); (iii) A realistic upper limit for *el-ph* interaction strength was earlier fixed at 600 meV; and (iv) Range of validity of BCS-MF theory requires that $\lambda < 0.25$. These conditions enforce severe constraints on the parameters g , ω , D_o , and U for which the system can undergo superconducting instability and if that happens on the achievable T_c 's. The variation of Δ_α (at $T = 0$) with δ is shown in Figs. 4-6, for different values of ω , D_o , and g , respectively. Since the trends are similar for Δ_α and T_c , we will discuss the T_c curves shown in Figs. 7-9. The lower limit of δ for the curves in Figs. 4-9 is determined by the condition on λ , and the upper cut-off as a function of δ enforces the small polaron condition. The variation of T_c with δ for various values of ω is shown in Fig. 7. For fixed U , D_o and g , BCS-MF superconductivity is confined to the ω range: $\omega_{min} < \omega < \omega_{max}$ where $\omega_{min} = U/2g^2$ and $\omega_{max} = \omega_{min} + (0.25q(n)D_P/2g^2)$. In this allowed range of ω , moderate values of T_c are possible. Increasing ω is found to increase the T_c 's achievable and expands the density range in which superconductivity is possible. The variation of T_c with δ for different values of D_o is shown in Fig. 8, and it shows that in the range shown changes in D_o do not have much effect. On the other hand, the T_c vs. δ curves shown in Fig. 9 show that small changes in g severely narrow the range of δ for which superconductivity is possible. It is clear that the various conditions mentioned earlier severely limit the range of δ for which superconductivity is possible and the values of T_c 's achievable. We would also like to note that below the lower cut-off of δ for each curve in the Figs. 4-9, the λ moves out of the BCS-MF regime into the intermediate to strong coupling regime and whether superconductivity is possible in that range of δ cannot be addressed using the weak coupling formulas used in this

section. The values of U , g , D_o , and ω used in making the T_c estimates are definitely not unrealistic considering the variety of molecules synthesizable and crystallizable. Though band-filling control has not yet been achieved in molecular conductors, such a possibility cannot be ruled out in the future. Even if band-filling control is not possible, our results show that JT polarons can undergo superconducting instability with moderate T_c 's in a realistic range of U , g , D_o , and ω realizable in molecular conductors. This completes the analysis of superconductivity in the BCS-MF regime of our model. In the next section, we consider the strong coupling regime (the Bose regime) of U_A .

IV. BOSE CONDENSATION IN THE STRONG COUPLING REGIME OF U_A

In this regime, all the JT polarons are in paired states below a temperature of $O(|U_A|)$. To obtain the Bose condensation temperature of these pre-formed pairs, we start from the Hamiltonian H_P [see Eq. (13)]. Since the largest terms in H_P are H_R and H_A (in the strong coupling regime), we treat $(H_R + H_A)$ as the part which determines the ground state energy and take H_{KE}^P as a perturbation. Now, in the ground state of $(H_R + H_A)$, a site has either a singlet occupying one of the orbitals or is empty. The *interorbital* pairs are projected out because of the strong *interorbital* repulsion (U_R). When we switch on the hopping term (H_{KE}^P), the pairs become mobile through a second order (in H_{KE}^P) process. For the ground state of $(H_R + H_A)$ we have

$$(H_R + H_A)|p\rangle = E_o|p\rangle, \quad (37)$$

where $E_o = (-|U_A|/2) \sum_{j\alpha\sigma} n_{j\alpha\sigma}$ is the ground state energy. The second order pair hopping term then is,

$$E_2 = -\frac{t_P^2}{|U_A|} \sum_r \langle p | \sum_{ij} \sum_{\alpha\sigma} c_{i\alpha\sigma}^\dagger c_{j\alpha\sigma} | r \rangle \langle r | \\ \times \sum_{lm} \sum_{\beta\sigma'} c_{l\beta\sigma'}^\dagger c_{m\beta\sigma'} | p \rangle. \quad (38)$$

In Eq. (38), the r sum is over states other than the degenerate ground states. Since $\sum_r |r\rangle\langle r| = I - \sum_p |p\rangle\langle p|$ and noting that $\langle p | T | p' \rangle = 0$, the second order term becomes

$$E_2 = -\frac{t_P^2}{|U_A|} \langle p | \sum_{ij} \sum_{\alpha\sigma} c_{i\alpha\sigma}^\dagger c_{j\alpha\sigma} \sum_{lm} \sum_{\beta\sigma'} c_{l\beta\sigma'}^\dagger c_{m\beta\sigma'} | p \rangle. \quad (39)$$

The E_2 is non-zero for (A) $l = j$; $i = m$; $\alpha = \beta$; $\sigma = \sigma'$ or (B) $i = l$; $j = m$; $\alpha = \beta$; $\sigma = -\sigma'$. Then,

$$E_2 = -\frac{t_P^2}{|U_A|} (\langle p | 2 \sum_{ij\alpha} c_{i\alpha\uparrow}^\dagger c_{i\alpha\downarrow}^\dagger c_{j\alpha\downarrow} c_{j\alpha\uparrow} | p \rangle \\ + \langle p | \sum_{ij\alpha} c_{i\alpha\sigma}^\dagger c_{j\alpha\sigma} c_{j\alpha\sigma}^\dagger c_{i\alpha\sigma} | p \rangle). \quad (40)$$

The hopping processes corresponding to the first and second terms in E_2 are shown in Fig. 10. E_2 can be calculated considering the probability amplitudes for the processes shown in the figure and we obtained it to be the ground state energy of the Hamiltonian

$$H_B = -2 \frac{t_P^2 \bar{q}(n)}{|U_A|} \sum_{ij\alpha} c_{i\alpha\uparrow}^\dagger c_{i\alpha\downarrow}^\dagger c_{j\alpha\downarrow} c_{j\alpha\uparrow} \\ + \frac{t_P^2 \bar{q}(n)}{|U_A|} \sum_{ij} \sum_{\alpha\sigma} n_{i\alpha\sigma} n_{j\alpha\sigma} - \frac{Z t_P^2 \bar{q}(n)}{|U_A|} \sum_{j\alpha\sigma} n_{j\alpha\sigma}, \quad (41)$$

where $\bar{q}(n) = (1 - n/2)/(1 - n/4)$ is the Gutzwiller projection factor and Z is the co-ordination number of a site in the lattice. The Bose condensation temperature (T_B) in the strong coupling regime of a three dimensional non-degenerate attractive Hubbard model was obtained in Ref.²⁷. Comparing our results with theirs, one can immediately write down the T_B for our case, and it is

$$k_B T_B = \frac{2(n-2)\bar{q}(n)Zt_P^2}{2|U_A| \ln(\frac{n}{4-n})}. \quad (42)$$

The above formula is relevant for $|U_A|/(\sqrt{\bar{q}(n)}t_P) \geq 12$. Here it must be pointed out that the finite temperature analysis in this section was done in real space and hence one need not worry about the orthogonality of the Gutzwiller projected excited state wave functions obtained by varying the occupation numbers $n_{k\alpha\sigma}$, as was done in Ref.²⁶. Note that for $n = 2$, we have a Mott insulator and T_B is zero. While making T_B estimates, we have to again satisfy the constraints (i)-(iii) given in the previous section. The small polaron formation condition in the strong coupling regime is $g^2\omega > \sqrt{\bar{q}(n)}D_o$ where D_o is the original half-band-width equal to $6t$ for a simple cubic lattice we have considered. The variation of T_B as a function of δ for various values of ω is shown in Fig. 11, and it is seen that decreasing ω increases the T_B 's and contracts the range of δ in which Bose condensation is possible. The upper cut-off in Figs. 11-13 is due to the violation of the small polaron condition. In Fig. 12, we have displayed T_B vs. δ for different values of D_o . Decreasing D_o decreases T_B while expanding the δ range for Bose condensation. Finally, T_B vs. δ for various values of g is shown in Fig. 13. Increase of g is seen to sharply reduce T_B . Overall, it is clear from the figures that T_B 's up to 100 K can be possible in the strong coupling regime. Furthermore, we note that slightly higher values of T_B can be obtained in the intermediate coupling regime as compared to the strong coupling regime threshold ($|U|/t \approx 12$) (see Fig. 2 in Ref.²⁵).

V. THE MOTT INSULATOR WITH SINGLETS

We have noted earlier that the ground state of the Hamiltonian H_P is a Mott insulator for the case of two electrons per site. This Mott insulating state obtains independent of the value of U_A (< 0) (see also the note in Ref.²⁸). The insulating state is obtained because of the strong *interorbital* repulsion U_R between the JT polarons. The repulsion U_R narrows the polaron band as the density increases and eventually drives it zero at $n = 2$. Now, due to the presence of finite *intraorbital* attraction between the polarons, the insulating state has a polaron singlet occupying one of the orbitals on site. Since the singlet can occupy either of the two orbitals available on a site, the insulating ground state is highly degenerate when U_R is infinity. When U_R is large and finite, a pair on a site can gain energy by virtual hopping to a nearest neighbor vacant orbital. This gain in energy, in second order perturbation theory, is $(-Zt_P^2)/(2U_R + |U_A|)$ per polaron. Hence for finite and large U_R the degeneracy of the insulating state reduces to two and the singlets order in alternate orbitals on NN sites and thus we have an Orbital Density Wave state. We also note that one can map the paired polaron Mott insulator to an Ising model since at each site the pair could be in either of the orbitals. Assigning pseudo-spins \uparrow to occupation of orbital 1 and \downarrow to that of orbital 2, the Ising model is $H = \sum_{\langle i,j \rangle} JS_i S_j$ with $J = t_P^2/(2U_R + |U_A|)$. The ground state corresponds to the orbitally antiferromagnetic state mentioned earlier. When the electron density deviates from $n = 2$, the insulator undergoes an insulator to metal transition and the superconducting instability of this metallic state was analyzed in the previous sections.

VI. CONCLUSIONS

In this paper we presented a theoretical study of superconductivity in a three dimensional molecular conductor in which the molecular orbitals participating in the conduction band formation are doubly degenerate and EMVC for electrons in these orbitals interacting with non-degenerate *intramolecular* vibration mode is large enough to lead to the formation of Jahn-Teller (JT) small polarons. We argued that the effective polaron-polaron interaction can be attractive for material parameters realizable in molecular conductors, and this interaction is the source of superconductivity in our model. On analyzing superconducting instability in the weak and strong coupling regimes of this attractive interaction, we found that superconducting transition temperatures up to 100 K are achievable in molecular conductors within this mechanism. We also find, for two particles per molecular site, that the ground state is a novel Mott insulating state in which a polaron singlet occupies one of the doubly degenerate orbitals on each site. In the infinite

interorbital repulsion case, this Mott insulator is highly degenerate since the singlet has the freedom to occupy either of the orbitals on a site. On the other hand, in the case of large but finite *interorbital* repulsion case, we found that the degeneracy of the ground state is reduced to two with the singlets orbitally antiferromagnetically ordered. When the number of particles per site deviates from two, the Mott insulator undergoes an insulator to metal transition.

ACKNOWLEDGMENTS

One of the authors (S. Y.) would like to thank Sanjoy Datta for useful discussions.

APPENDIX A

Here we show that, for strong coupling (*i.e.*, $2G/\omega \gg 1$), $E \otimes e$ JT model is equivalent to the $E \otimes \beta$ model in Eq. (1). For $E \otimes e$,

$$H = t \sum_{ij} \sum_{\alpha\sigma} d_{i\alpha\sigma}^\dagger d_{j\alpha\sigma} + \frac{M\omega^2}{2} \sum_{i\alpha} Q_{i\alpha}^2 + \frac{M}{2} \sum_{i\alpha} \dot{Q}_{i\alpha}^2 - G\sqrt{2M\omega} \sum_{i\sigma} \begin{pmatrix} d_{i1\sigma}^\dagger & d_{i2\sigma}^\dagger \end{pmatrix} \begin{pmatrix} Q_{1i} & Q_{2i} \\ Q_{2i} & -Q_{1i} \end{pmatrix} \begin{pmatrix} d_{i1\sigma} \\ d_{i2\sigma} \end{pmatrix} + U \sum_{j\alpha} n_{j\alpha\uparrow} n_{j\alpha\downarrow} + U \sum_{j\sigma\sigma'} n_{j1\sigma} n_{j2\sigma'}. \quad (\text{A1})$$

Now we do a rotation transformation on H . For this purpose, let

$$- \begin{pmatrix} Q_{1i} & Q_{2i} \\ Q_{2i} & -Q_{1i} \end{pmatrix} = Q_i \begin{pmatrix} -\cos(\theta_i) & \sin(\theta_i) \\ \sin(\theta_i) & \cos(\theta_i) \end{pmatrix}, \quad (\text{A2})$$

where $Q_i = \sqrt{Q_{1i}^2 + Q_{2i}^2}$ and

$$\begin{pmatrix} c_{i1\sigma} \\ c_{i2\sigma} \end{pmatrix} = \begin{pmatrix} \sin(\frac{\theta_i}{2}) & \cos(\frac{\theta_i}{2}) \\ \cos(\frac{\theta_i}{2}) & -\sin(\frac{\theta_i}{2}) \end{pmatrix} \begin{pmatrix} d_{i1\sigma} \\ d_{i2\sigma} \end{pmatrix}. \quad (\text{A3})$$

Using the above, H is transformed to:

$$H = t \sum_{ij\sigma} \begin{pmatrix} c_{i1\sigma}^\dagger & c_{i2\sigma}^\dagger \end{pmatrix} \begin{pmatrix} 1 & 0 \\ 0 & 1 \end{pmatrix} \begin{pmatrix} c_{j1\sigma} \\ c_{j2\sigma} \end{pmatrix} + G\sqrt{2M\omega} \sum_{i\sigma} \begin{pmatrix} c_{i1\sigma}^\dagger & c_{i2\sigma}^\dagger \end{pmatrix} \begin{pmatrix} Q_i & 0 \\ 0 & -Q_i \end{pmatrix} \begin{pmatrix} c_{i1\sigma} \\ c_{i2\sigma} \end{pmatrix} + \frac{M\omega^2}{2} \sum_i Q_i^2 + \frac{1}{2M} \sum_i \left(\frac{\partial^2}{\partial Q_i^2} + \frac{1}{Q_i} \frac{\partial}{\partial Q_i} + \frac{1}{Q_i^2} \frac{\partial^2}{\partial \theta_i^2} \right) + U \sum_{j\alpha} n_{j\alpha\uparrow} n_{j\alpha\downarrow} + U \sum_{j\sigma\sigma'} n_{j1\sigma} n_{j2\sigma'}. \quad (\text{A4})$$

As argued in Ref.¹⁵, for $2G/\omega \gg 1$, $(1/Q_i)(\partial/\partial Q_i)$ and $(1/Q_i^2)(\partial^2/\partial \theta_i^2)$ are unimportant, and we are left

with an effective single mode equation. Then using $\sqrt{2M\omega}Q_i = b_i + b_i^\dagger$, one gets the Eq. (1) given in the text. Here it should be pointed out that the single normal mode approximation for $E \otimes e$ works only for the low lying excitations of the mode. For the transition temperatures obtained and the frequencies considered $\omega/k_B T_c \gg 1$, and hence phonon averaging after the Lang-Firsov transformation yields for the single mode approximated $E \otimes e$ system the same result given by Eq. (15) in the text.

-
- ¹ D. Jerome, A. Mazaud, M. Ribault, and K. Bechgaard, J. Phys. (France) Lett. **41**, L95(1980).
² K. Bechgaard, C. S. Jacobsen, K. Mortensen, H. J. Pedersen, and N. Thorup, Solid State. Commun. **33**, 1119(1980).
³ T. Ishiguro, K. Yamaji, and G. Saito, *Organic Superconductors* (Springer, Berlin, 1998).
⁴ W. A. Little, Phys. Rev. **134**, A1416(1964).
⁵ D. Jerome, Science **252**, 1509(1991).
⁶ A. J. Heeger, Rev. Mod. Phys. **73**, 681(2001).
⁷ J. Bardeen, L. N. Cooper, and J. R. Schrieffer, Phys. Rev. **108**, 1175(1957).
⁸ A. J. Berlinsky, J. F. Carolan, and L. Weiler, Solid State Commun. **15**, 795(1974); N. O. Lipari, M. J. Rice, C. B. Duke, R. Bozio, A. Girlando, and C. Pecile, Intl. J. Quan. Chem. QM Symp. **11**, 583(1977); K. Yamaji, Solid State. Commun. **61**, 413(1987); J. C. R. Faulhaber, D. K. K. Ko, and P. R. Briddon, Syn. Met. **60**, 227(1993); V. M. Yartsev and A. Graja, Intl. J. Mod. Phys. B **12**, 1643(1998); A. Devos and M. Lannoo, Phys. Rev. B **58**, 8236(1998); T. Kato and T. Yamabe, J. Chem. Phys. **115**, 8592(2001); T. Kato, K. Yozhizawa, and K. Hirao, J. Chem. Phys. **116**, 3420(2002); J. Sinoa, J. Schliemann, A. S. Núñez, and A. H. MacDonald, Phys. Rev. Lett. **87**, 226802(2001); C. M. Varma, J. Zannen, and K. Raghavachari, Science **254**, 989(1991); V. P. Ansharov, O. Gunnarson, and A. I. Liechtenstein, Phys. Rev. B **48**, 7651(1993); O. Gunnarson, Rev. Mod. Phys. **69**, 575(1997); M. Cote, J. S. Grossmann, M. L. Cohen, and S. G. Louie, Phys. Rev. Lett. **81**, 697(1998).
⁹ R. Ramakumar, Y. Tanaka, and K. Yamaji, Phys. Rev. B **56**, 795(1997); R. Ramakumar and K. Yamaji, Eur. Phys. J. B **24**, 71(2001).
¹⁰ J. Appel, in *Solid State Physics*, Vol. 21, eds. H. Ehrenreich, F. Seitz, and D. Turnbull (Academic Press, New York, 1967), p193; A. S. Alexandrov and N. F. Mott, *Polarons and Bipolarons* (World Scientific, Singapore, 1995).
¹¹ A. B. Migdal, Zh. Eksp. Teor. Fiz. **34**, 1438(1958)[Sov. Phys. JETP **34**, 996(1958)].
¹² G. M. Eliashberg, Zh. Eksp. Teor. Fiz. **38**, 966(1960) [Sov. Phys. JETP **11**, 696(1960)]; **39**, 1437(1960)[**12**, 1000(1961)].
¹³ T. Holstein, Ann. Phys. (N. Y.) **8**, 325(1959); **8**, 343(1959).
¹⁴ R. Ramakumar and S. Yarlagadda, Phys. Rev. B **67**, 214502(2003).

- ¹⁵ M. D. Sturge, in *Solid State Physics*, Vol. 20, eds. H. Ehrenreich, F. Seitz, and D. Turnbull (Academic Press, New York, 1967), p 91.
¹⁶ S. El Shawish, J. Bonča, Li-Chung Ku, and S. A. Trugman, Phys. Rev. B **67**, 014301(2003).
¹⁷ I. G. Lang and Yu. A. Firsov, Zh. Eksp. Teor. Fiz. **43**, 1843(1962) [Sov. Phys. JETP **16**, 1301(1962)].
¹⁸ M. C. Gutzwiller, Phys. Rev. Lett. **10**, 159(1963); Phys. Rev. **134**, A923(1964).
¹⁹ S. Yarlagadda, Phys. Rev. B **62**, 14828(2000).
²⁰ T. Kato and T. Yamabe in Ref⁸.
²¹ T. Okabe, J. Phys. Soc. of Japan **65**, 1056(1996).
²² F. C. Zhang, C. Gros, T. M. Rice, and H. Shiba, Supercond. Sci. Technol. **1**, 36(1988).
²³ R. Micnas, J. Ranninger, and S. Robaszkiewicz, Rev. Mod. Phys. **62**, 113(1990).
²⁴ M. Keller, W. Metzner, and U. Schollwöck, Phys. Rev. Lett. **86**, 4612(2001).
²⁵ A. Sewer, X. Zotos, and H. Beck, Phys. Rev. B **66**, 140504(2002).
²⁶ The reader may be concerned about the validity of calculating T_c from a theory on an effective Hamiltonian obtained using Gutzwiller approximation. Since BCS-MF T_c is much smaller than the effective Fermi temperature, the corrections brought about by the modification required in the occupation number ($n_{k\alpha\sigma}$) to incorporate the finite temperature effects in Gutzwiller projection is expected to be small. See: T. M. Rice, K. Ueda, H. R. Ott, and H. Rudigier, Phys. Rev. B **31**, 594(1985); K. Seiler, C. Gros, T. M. Rice, K. Ueda, and D. Vollhardt, J. Low. Temp. Phys. **64**, 195(1986).
²⁷ S. Robaszkiewicz, R. Micnas, and K. A. Chao, Phys. Rev. B **23**, 1447(1981).
²⁸ For $n = 2$, a Mott insulating state is also possible for $0 \leq U_A \ll U_R$.

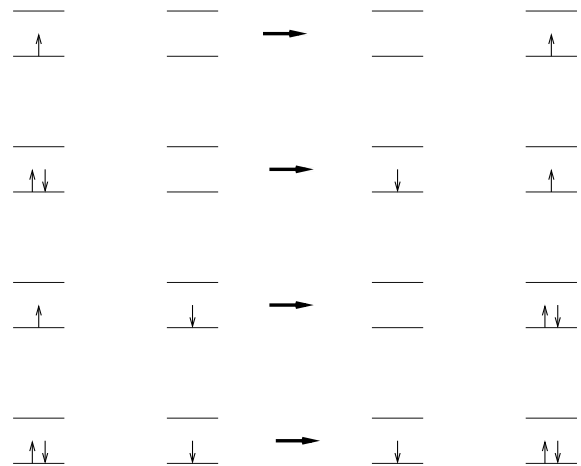


FIG. 1. The inter-site hopping processes considered (see text).

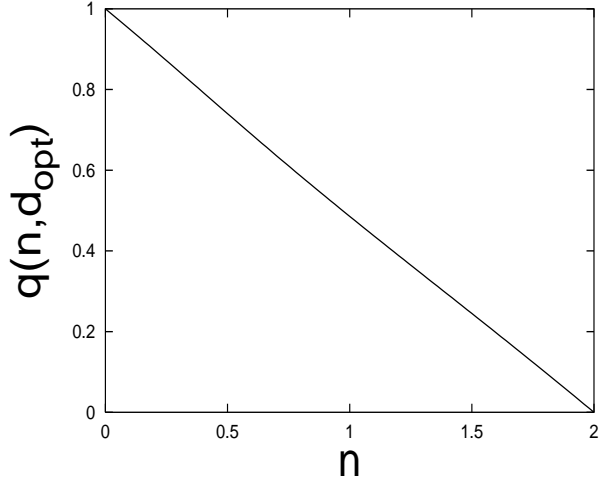


FIG. 2. The variation of the band-width renormalization factor as a function of particle density.

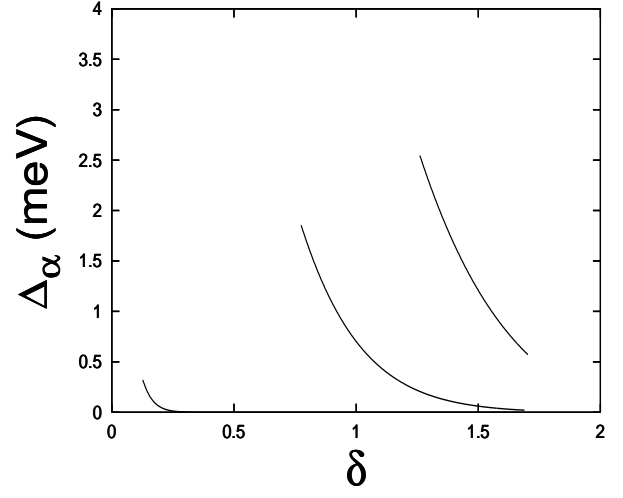


FIG. 4. Δ_α vs. δ for various values of ω (in eV): 0.348 (left), 0.352 (middle), 0.355 (right). Values of the other parameters are: $U = 1$ eV, $D_o = 0.6$ eV, and $g = 1.2$.

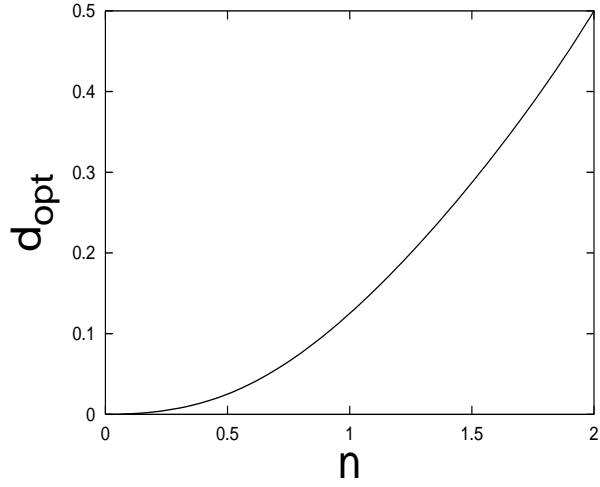


FIG. 3. The variation of the *intraorbital* double occupancy as a function of particle density.

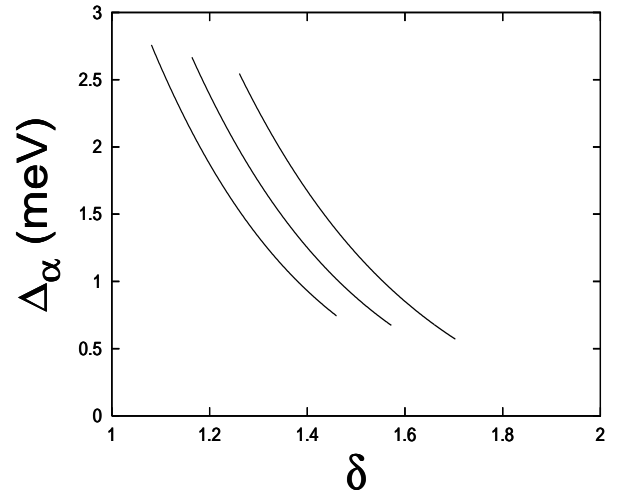


FIG. 5. Δ_α vs. δ for various values of D_o (in eV): 0.70 (left), 0.65 (middle), 0.60 (right). Values of the other parameters are: $U = 1$ eV, $\omega = 0.355$ eV, and $g = 1.2$.

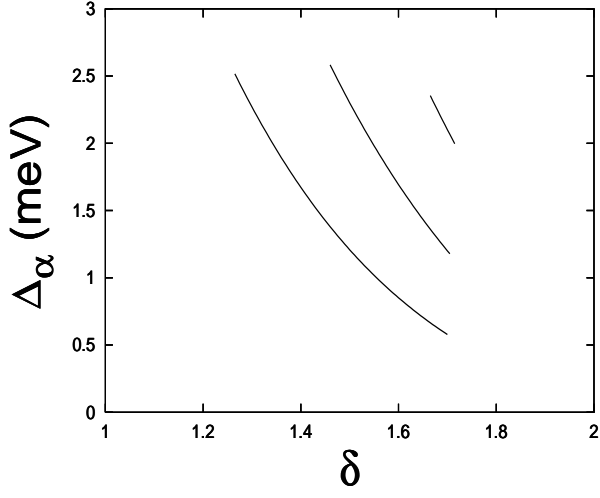


FIG. 6. Δ_α vs. δ for various values of g : 1.200 (left), 1.202 (middle), 1.204 (right). Values of the other parameters are (in eV): $U = 1$, $\omega = 0.355$, and $D_o = 0.6$.

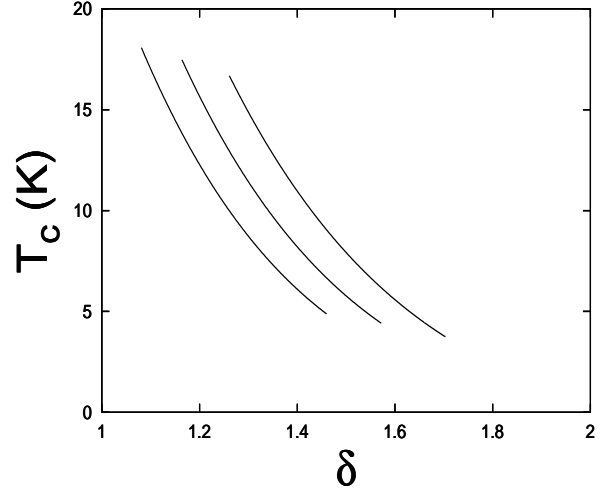


FIG. 8. T_c vs. δ for various values of D_o (in eV): 0.70 (left), 0.65 (middle), 0.60 (right). Values of the other parameters are: $U = 1$ eV, $\omega = 0.355$ eV, and $g = 1.2$.

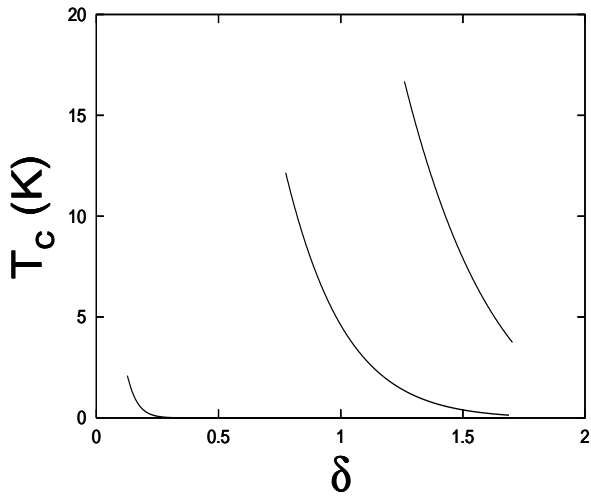


FIG. 7. T_c vs. δ for various values of ω (in eV): 0.348 (left), 0.352 (middle), 0.355 (right). Values of the other parameters are: $U = 1$ eV, $D_o = 0.6$ eV, and $g = 1.2$.

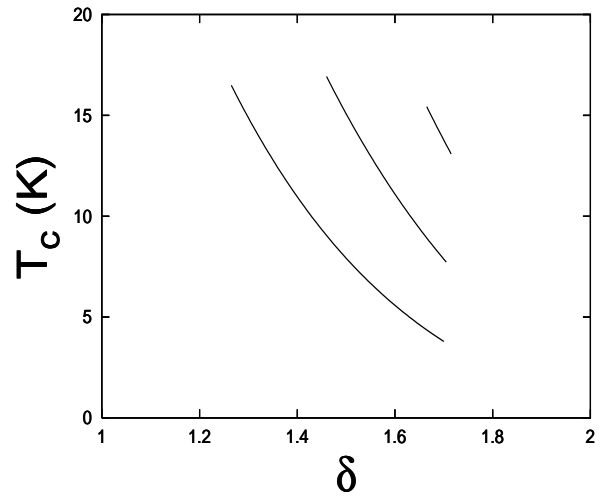


FIG. 9. T_c vs. δ for various values of g : 1.200 (left), 1.202 (middle), 1.204 (right). Values of the other parameters are (in eV): $U = 1$, $\omega = 0.355$, and $D_o = 0.6$.

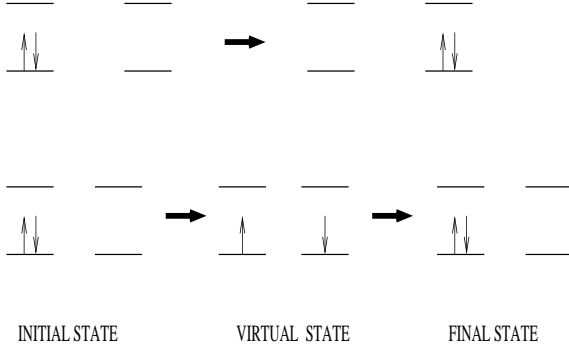


FIG. 10. The inter-site hopping processes (see text) in the Bose regime.

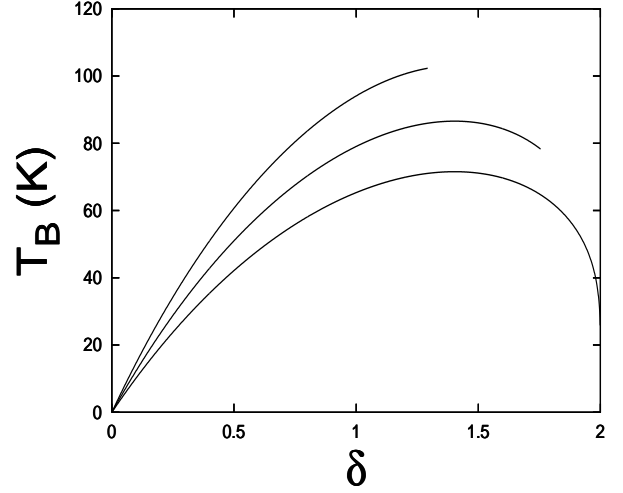


FIG. 12. T_B vs. δ for various values of D_o (in eV): 0.60 (top), 0.55 (middle), 0.50 (bottom). Values of the other parameters are: $U = 0.9$ eV, $\omega = 0.4$ eV, and $g = 1.2$.

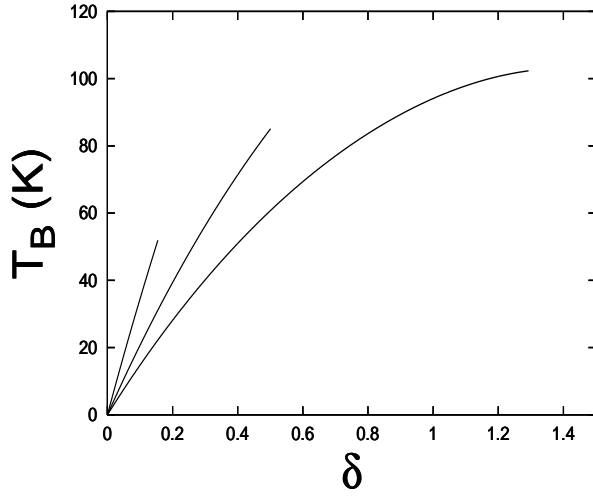


FIG. 11. T_B vs. δ for various values of ω (in eV): 0.350 (left), 0.375 (middle), 0.400 (right). Values of the other parameters are: $U = 0.9$ eV, $D_o = 0.6$ eV, and $g = 1.2$.

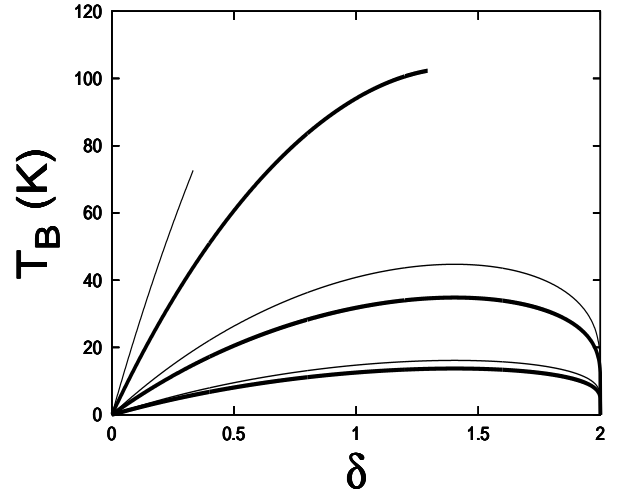


FIG. 13. T_B vs. δ for various values of g : 1.20 (top), 1.3 (middle), 1.4 (bottom). Values of the other parameters are (in eV): $U = 0.9$ (thick lines) and $U = 1.0$ (thin lines), $\omega = 0.4$, and $D_o = 0.6$.